Optical spectroscopic observations of gamma-ray blazars candidates I: preliminary results

Share Your Story

The Harvard community has made this article openly available.
Please share how this access benefits you. Submit a story .

Accessibility

Optical spectroscopic observations of gamma-ray blazars candidates I: preliminary results

A. Paggi[1], D. Milisavljevic[1], N. Masetti[2], E. Jiménez-Bailón[3], V. Chavushyan[4], R. D'Abrusco[1], F. Massaro[5], M. Giroletti[2], H. A. Smith[1], R. Margutti[1], G. Tosti[6], J. R. Martinez Galarza[1], H. Otí-Floranes[3], M. Landoni[7,8,1], J. E. Grindlay[1], S. Funk[5]

version April 22, 2014: fm

[1]Harvard-Smithsonian Center for Astrophysics, 60 Garden Street, Cambridge, MA 02138, USA

[2]INAF - Istituto di Astrosica Spaziale e Fisica Cosmica di Bologna, via Gobetti 101, 40129, Bologna, Italy

[3]Instituto de Astronomía, Universidad Nacional Autónoma de México, Apdo. Postal 877, Ensenada, 22800 Baja California, México

[4]Instituto Nacional de Astrofísica, Óptica y Electrónica, Apartado Postal 51-216, 72000 Puebla, México

[5]SLAC - National Laboratory and Kavli Institute for Particle Astrophysics and Cosmology, 2575 Sand Hill Road, Menlo Park, CA 94025, USA

[6]Dipartimento di Fisica, Università degli Studi di Perugia, 06123 Perugia, Italy

[7]INAF - Osservatorio Astronomico di Brera, Via Emilio Bianchi 46, I-23807 Merate, Italy

[8]INFN - Istituto Nazionale di Fisica Nucleare, sede di Milano Bicocca, Piazza della Scienza, 3, 20126 Milano, Italy

ABSTRACT

A significant fraction ($\sim 30\%$) of the gamma-ray sources listed in the second *Fermi* LAT (2FGL) catalog is still of unknown origin, being not yet associated with counterparts at lower energies. Using the available information at lower energies and optical spectroscopy on the selected counterparts of these gamma-ray objects we can pinpoint their exact nature. Here we present a pilot project pointing to assess the effectiveness of the several classification methods developed to select gamma-ray blazar candidates. To this end, we report optical spectroscopic observations of a sample of 5 gamma-ray blazar candidates selected on the basis of their infrared WISE colors or of their low-frequency radio properties. Blazars come in two main classes: BL Lacs and FSRQs, showing similar optical spectra except for the stronger emission lines of the latter. For three of our sources the almost featureless optical spectra obtained confirm their BL Lac nature, while for the source WISEJ022051.24+250927.6 we observe emission lines with equivalent width $EW \sim 31$ Å, identifying it as a FSRQ with $z = 0.48$. The source WISEJ064459.38+603131.7, although not featuring a clear radio counterpart, shows a blazar-like spectrum with weak emission lines with $EW \sim 7$ Å, yielding a redshift estimate of $z = 0.36$. In addition we report optical spectroscopic observations of 4 WISE sources associated with known gamma-ray blazars without a firm classification or redshift estimate. For all of these latter sources we confirm a BL Lac classification, with a tentative redshift estimate for the source WISEJ100800.81+062121.2 of $z = 0.65$.

Subject headings: galaxies: active - galaxies: BL Lacertae objects - radiation mechanisms: non-thermal

1. Introduction

About 1/3 of the γ-ray sources listed in the 2nd *Fermi* catalog (2FGL, Nolan et al. 2012) have not yet been associated with counterparts at lower energies. A precise knowledge of the number of unidentified gamma-ray sources (UGSs) is extremely relevant since for example it could help to provide the tightest constraint on the dark matter models ever determined (Abdo et al. 2013). Many UGSs could be blazars, the largest identified population of extragalactic γ-ray sources, but how many are actually blazars is not yet known due in part to the incompleteness of the catalogs used for the associations (Ackermann et al. 2011). The first step to reduce the number of UGSs is therefore to recognize those that could be blazars.

Blazars are the rarest class of Active Galactic Nuclei, dominated by variable, non-thermal radiation over the entire electromagnetic spectrum (e.g., Urry & Padovani 1995; Giommi, Padovani, & Polenta 2013). Their observational properties are generally interpreted in terms of a relativistic jet aligned within a small angle to our line of sight (Blandford & Rees 1978).

Blazars have been classified as BL Lacs and FSRQs (or BZBs and BZQs according to the nomenclature proposed by Massaro et al. 2013), with the latter showing similar optical spectra except for the stronger emission lines, as well as higher radio polarization. In particular, if the only spectral features observed are emission lines with rest frame equivalent width $EW \leq 5$ Å the object is classified as a BZB (Stickel et al. 1991; Stocke & Rector 1997), otherwise it is classified as BZQ (Laurent-Muehleisen et al. 1999; Massaro et al. 2013). Systematic projects aimed at obtaining optical spectroscopic observations of blazars are currently carried out by different groups (see, e.g., Sbarufatti et al. 2006, 2009; Landoni et al. 2012, 2013[1]; Shaw et al. 2013).

The blazar spectral energy distributions (SEDs) typically show two peaks: one in the range of radio - soft X-rays, due to synchrotron emission by highly relativistic electrons within the jet;

---

[1] http://archive.oapd.inaf.it/Wallace/index.html

and another one at hard X-ray or γ-ray energies, interpreted as inverse Compton upscattering by the same electrons of the seed photons provided by the synchrotron emission (Inoue & Takahara 1996) with the possible addition of seed photons from outside the jets yielding contributions to the non-thermal radiations due to external inverse Compton scattering (see Dermer & Schlickeiser 1993; Dermer et al. 2009) often dominating the γ-ray outputs (Aharonian et al. 2009; Ackermann et al. 2011).

Recently, D'Abrusco et al. (2013) proposed an association procedure to recognize γ-ray blazar candidates on the basis of their positions in the three-dimensional WISE color space. As a matter of fact, blazars - whose emission is dominated by beamed, non thermal emission - occupy a defined region in such a space, well separated from that occupied by other sources in which thermal emission prevails (Massaro et al. 2011b; D'Abrusco et al. 2012). Applying this method, Cowperthwaite et al. (2013) recently identified thirteen gamma-ray emitting blazar candidates from a sample of 102 previously unidentified sources selected from Astronomer's Telegrams and the literature.

Massaro et al. (2013a) applied the classification method proposed by D'Abrusco et al. (2013) to 258 UGSs and 210 active galaxies of uncertain type (AGUs) listed in the 2FGL (Nolan et al. 2012) finding candidate blazar counterparts for 141 UGSs and 125 AGUs. The classification method proposed by D'Abrusco et al. (2013), however, can only be applied to sources detected in all 4 WISE bands, i.e., 3.4, 4.6, 12 and 22 μm.

Using the X-ray emission in place of the 22 μm detection, Paggi et al. (2013) proposed a method to select γ-ray blazar candidates among *Swift*-XRT sources considering those that feature a WISE counterpart detected at least in the first 3 bands, and with IR colors compatible with the 90% two-dimensional densities of known γ-ray blazar evaluated using the Kernel Density Estimation (KDE) technique (see, e.g., Richards et al. 2004; D'Abrusco, Longo, & Walton 2009; Laurino et al. 2011, and reference therein), so selecting 37 new γ-ray blazar candidates. Similarly,

Table 1: WISE sources discussed in this paper. In the upper part of the Table we list the γ-ray blazar candidates associated with UGSs or AGUs, while in the lower part we list the sources associated with known γ-ray blazars. Column description is given in the main text (see Sect. 3).

WISE NAME	RA J2000	DEC J2000	OTHER NAME	NAME 2FGL	NOTES
J022051.24+250927.6	02:20:51.24	+25:09:27.6	NVSSJ022051+250926	2FGLJ0221.2+2516	UGS X-KDE
J050558.78+611335.9	05:05:58.79	+61:13:35.9	NVSSJ050558+611336	2FGLJ0505.9+6116	AGU WISE
J060102.86+383829.2	06:01:02.87	+38:38:29.2	WN0557.5+3838	2FGLJ0600.9+3839	UGS WENSS
J064459.38+603131.7	06:44:59.39	+60:31:31.8		2FGLJ0644.6+6034	UGS WISE
J104939.34+154837.8	10:49:39.35	+15:48:37.9	GB6J1049+1548	2FGLJ1049.4+1551	AGU R-KDE
J022239.60+430207.8	02:22:39.61	+43:02:07.9	BZBJ0222+4302	2FGLJ0222.6+4302	A, Z=0.444?
J100800.81+062121.2	10:08:00.82	+06:21:21.3	BZBJ1008+0621	2FGLJ1007.7+0621	B, CAND
J131443.81+234826.7	13:14:43.81	+23:48:26.8	BZBJ1314+2348	2FGLJ1314.6+2348	B, CAND
J172535.02+585140.0	17:25:35.03	+58:51:40.1	BZBJ1725+5851	2FGLJ1725.2+5853	B, CAND

using the radio emission as additional information, Massaro et al. (2013c) investigated all the radio sources in NVSS and SUMSS surveys that lie within positional uncertainty region of *Fermi* UGSs and, considering those sources with IR colors compatible with the 90% two-dimensional KDE densities of known γ-ray blazar, selected 66 additional γ-ray blazar candidates.

Finally, Massaro et al. (2013b) investigated the low-frequency radio emission of blazars and searched for sources with similar features combining the information derived from the WENSS and NVSS surveys, identifying 26 γ-ray candidate blazars in the *Fermi* LAT the positional uncertainty region of 21 UGSs.

In this paper we present a pilot project to assess the effectiveness of the three methods described before (position in the three dimensional WISE IR colors space, radio or X-ray detection plus position in the two dimensional WISE IR color space and low-frequency radio properties) in selecting gamma-ray blazar candidates. To this end, we report on optical spectra acquired using MMT, Loiano and OAN telescopes of 5 WISE γ-ray blazar candidates - counterparts of three UGSs and two AGUs - in order to identify their nature and to test the reliability of these different approaches in selecting γ-ray candidate blazars. In addition, we also present optical spectra of 4 known γ-ray blazars with uncertain redshift estimates or unknown classification (BZB vs BZQ,) (Ackermann et al. 2011; Nolan et al. 2012) with a WISE counterpart identified by D'Abrusco et al. (2013).

We note that our approach in selecting the targets for our observations is different from that adopted in other works (i.e. Shaw et al. 2013), that is, selecting the source closest to radio or optical coordinates. Our approach for the target selection, as reported in D'Abrusco et al. (2013), Massaro et al. (2013a), Paggi et al. (2013) and Massaro et al. (2013b), is the following:

a) For *Fermi* UGSs or AGUs, among all the sources inside the 95% LAT uncertainty region ($\sim$ 10') we select gamma-ray blazar candidates on the basis of their multi-wavelength properties (IR, radio+IR, X-ray+IR, low-frequency radio). As a consequence, our selected

targets are not necessarily the closest to optical or radio coordinates. They may - in principle - not even have a radio counterpart.

b) For known gamma-ray blazars D'Abrusco et al. (2013) associate to Roma-BZCAT (Massaro et al. 2013) sources the closest WISE source inside 3.3" selected on the basis of its WISE colors. So, even if the these source are spatially compatible with radio or optical coordinates due to the WISE PSF extension ($\sim$ 6" in W1 band and $\sim$ 12" in W4 band, Wright et al. 2010), we cannot a-priori be sure that this IR source is actually the blazar counterpart. Since the probability of having two different blazars in 3.3" is essentially 0 (the blazar density in the sky is about 1 source per 10 square degrees), if the selected WISE source does show a blazar spectrum we can be confident that this is indeed the IR blazar counterpart and that D'Abrusco et al. procedure correctly classified the WISE source.

The paper is structured as follows: in Sect. 2 we describe the observation procedures and the data reduction process adopted, in Sect. 3 we present our results on individual sources and discuss them in Sect. 4, while in Sect. 5 we present our conclusions.

Throughout this paper USNO-B magnitudes are reported as photographic magnitudes, SDSS magnitudes are reported in AB system, and 2MASS magnitudes are reported in VEGA system.

2. Observations

The spectroscopic observations for all sources with the exception of WISEJ022239.60+430207.8 and WISEJ104939.34+154837.8 were carried out during nights of January 17 and 18, 2013 with the 6.5 m Multiple Mirror Telescope (MMT) and its Blue Channel Spectrograph with a 300 gpm grating and a 2x180" slit, for a resolution of about 6.2 Å. The spectra covered about 4800 Å, centered on 5900 Å, and the 3072 x 1024 pixel ccd22 was used as a detector. For each target, we obtained a series of two spectra, with exposure times of 1800-2700 s and combined them

during the reduction process. We used helium-neon-argon calibration lamps before and after each exposure. A few spectroscopic standards were also observed and used to remove the spectral response and to fluxcalibrate the data.

The object WISEJ022239.60+430207.8 was observed spectroscopically with the 1.5-meter "G.D. Cassini" telescope in Loiano (Italy) equipped with the BFOSC spectrograph, which carries a 1300×1340 pixels EEV CCD. Two 1800-s spectroscopic frames were secured on 3 December 2012, with start times at 21:12 and 21:44 UT, respectively. Data were acquired using Grism #4 and with a slit width of 2″0, giving a nominal spectral coverage between 3500 and 8700 Å and a dispersion of 4.0 Å/pix. Wavelength calibration was obtained with Helium-Argon lamps.

Likewise, three optical spectra of 1800 s each of source WISEJ104939.34+154837.8 were secured with the 2.1-meter telescope of the Observatorio Astronómico Nacional (OAN) in San Pedro Mártir (México) on 2 May 2013 with mid-exposure time 04:58 UT. The telescope carries a Boller & Chivens spectrograph and a 1024x1024 pixels E2V-4240 CCD. A slit width 2″.5 was used. The spectrograph was tuned in the $\sim 4000 \div 8000$ Å range (grating 300 l/mm), with a resolution of 4 Å/pixel, which corresponds to 8 Å (FWHM). Data were wavelength calibrated using Copper-Helium-Neon-Argon lamps, while for flux calibration spectrophotometric standard stars were observed twice during every night of the observing run.

The data reduction was carried out using the IRAF package of NOAO including bias subtraction, spectroscopic flat fielding, optimal extraction of the spectra and interpolation of the wavelength solution. All spectra were reduced and calibrated employing standard techniques in IRAF and our own IDL routines (see, e.g., Matheson et al. 2008).

3. Results on individual sources

In Table 1 we list the WISE sources presented in this paper. In the upper part of the table we report the γ-ray blazar candidates associated with UGSs or AGUs; in particular, in the NAME 2FGL column we indicate the name of associated *Fermi* source, in the OTHER NAME column we indicate the relative radio counterpart and in the NOTES column we indicate with X-KDE, WISE, WENSS and R-KDE the source selected as γ-ray blazar candidate according to Paggi et al. (2013), Massaro et al. (2013a), Massaro et al. (2013b) and Massaro et al. (2013c), respectively. In the lower part of the Table we list the sources associated with known γ-ray blazars with the classification method proposed by D'Abrusco et al. (2013), with additional information from BZCAT catalog; in particular, for these sources in the OTHER NAME column we indicate the associated blazar name, and in the NOTES column we report the class depending on the probability of the WISE source to be compatible with the model of the WISE *Fermi* Blazar locus (D'Abrusco et al. 2013, see Sect. 4) and we indicate with CAND the sources listed as blazar candidates or the reported redshift estimate (see Massaro et al. 2011b).

Optical images of the fields containing these sources are presented in Fig. 1, while the extracted spectra are presented in Figs. 2 and 3. The main observational results are presented in Table 2, and a discussion for each individual target is given in the following sub-sections. For each WISE source we report the main properties of the closest sources found in major radio, IR and optical surveys (together with the centroid separation) to obtain additional information on the source nature[2].

---

[2]Although a proper counterpart identification would require more sophisticated techniques (see for example Brand et al. 2006) for the scope of this work we are simply presenting a list of counterparts associations only based on positional match. A detailed discussion of the spatial association procedure of blazar with IR and low frequency radio catalog has been performed by D'Abrusco et al. (2013), Massaro et al. (2013a) and Massaro et al. (2013b), as well as an estimation of the

3.1. WISEJ022051.24+250927.6

This source lies in the positional uncertainty region at 95% level of confidence of the *Fermi* UGS 2FGLJ0221.2+2516 as reported in the 2FGL catalog (Nolan et al. 2012), and it is associated with the NVSS (Condon et al. 1998) radio source NVSSJ022051+250926 with a $\sim 1''$ angular separation. The USNO-B (Monet et al. 2003) optical counterpart, at $\sim 0.1''$, features magnitudes B1=18.74 mag, R1=18.82 mag, B2=19.80 mag, R2=19.51 mag and I2=18.10 mag. Paggi et al. (2013) showed that this source is positionally consistent ($\sim 4.7''$) with the X-ray *Swift* source SWXRTJ022051.5+250930, featuring an unabsorbed flux $\sim 1.3 \times 10^{-13}$ erg cm^{-2} s^{-1}. On the basis of its position in the two dimensional WISE IR color space - that is the [3.4]-[4.6] vs [4.6]-[12] color plane - this source has been selected by the same authors as γ-ray blazar candidate. The spectrum of WISEJ022051.24+250927.6 presented in Fig. 2a clearly shows strong emission lines that we identify as broad Mg ɪɪ ($EW = 30.8 \pm 0.7$ Å), narrow [Ne v] ($EW = 1.8 \pm 0.3$ Å), narrow [O ɪɪ] ($EW = 1.7 \pm 0.3$ Å), narrow [Ne ɪɪɪ] ($EW = 1.1 \pm 0.4$ Å) and narrow [O ɪɪɪ] ($EW = 15.8 \pm 0.3$ Å), yielding a redshift $z = 0.4818 \pm 0.0002$.

3.2. WISEJ050558.78+611335.9

The *Fermi* AGU 2FGLJ0505.9+6116 has been associated with the gamma-ray blazar candidate WISEJ050558.78+611335.9 by Massaro et al. (2013a). The WISE source is associated with the radio sources NVSSJ050558+611336 ($\sim 0.5''$) and WENSS (Rengelink et al. 1997) WN0501.4+6109 ($\sim 2.3''$). The closest source in the USNO-B catalog ($\sim 0.4''$ from WISE source, $\sim 0.1''$ from NVSS source) features magnitudes R1=18.71 mag, B2=20.73 mag, R2=18.67 mag and I2=17.30 mag, while the closest counterpart in the SDSS (Pâris et al. 2012; Ahn et al.

---

chance of spurious associations, that has also been discussed by Paggi et al. (2013) for the X-ray IR case.

2013) survey is SDSSJ050558.78+611335.8 ($\sim 0.1''$ from WISE source, $\sim 0.4''$ from NVSS source) with magnitudes u=21.66 mag, g=20.58 mag, r=19.65 mag, i=19.02 mag and z=18.58 mag. WISEJ050558.78+611335.9 is also associated with the 2MASS (Skrutskie et al. 2006) IR counterpart 2MASSJ05055874+6113359 ($\sim 0.1''$) with magnitudes H=16.228 mag and K=15.156 mag, with a lower limit on the J magnitude of 17.136 mag. The optical source J0505+6113 ($\sim 0.4''$) has been observed with Marcario Low Resolution Spectrograph on the Hobby-Eberly Telescope (Shaw et al. 2013), yielding a featureless spectrum that did not allow a redshift estimate. The 2LAC source coordinates for 2FGLJ0505.9+6116 are closer to the USNO ($\sim 0.2''$) source than to the SDSS source ($\sim 0.3''$). Although the latter optical sources, at a separation $\sim 0.4''$, are marginally consistent with each other - considering the astrometric uncertainties of $0.2''$ for USNO-B catalog and $0.1''$ for SDSS - it is likely that Shaw et al. observed the closest, brighter USNO source. According to the source position in the three dimensional WISE IR color space, this source has been selected by Massaro et al. (2013a) as γ-ray BZB candidate, and its featureless spectrum shown in Figure 2b confirms this classification of the WISE source. The similarly featureless spectrum shown by Shaw et al. features comparable fluxes but a different spectral shape, which is not unexpected due to the blazar strong optical variability (Bauer et al. 2009).

3.3.   WISEJ060102.86+383829.2

The *Fermi* UGS 2FGLJ0600.9+3839 has been associated with the gamma-ray blazar candidate WISEJ060102.86+383829.2 by Massaro et al. (2013a). The correspondent optical counterpart in the USNO-B catalog, at $\sim 0.1''$, features magnitudes R1=19.11 mag, R2=19.84 mag and I2=18.48 mag. According to Paggi et al. (2013) this source is positionally consistent ($\sim 0.6''$) with the X-ray *Swift* source SWXRTJ060102.8+383829 having a $0.3 - 10$ keV unabsorbed flux $\sim 2.3 \times 10^{-13}$ erg cm^{-2} s^{-1}. It is also associated with the radio sources NVSSJ060102+383828 ($\sim 0.5''$) and WN0557.5+3838 ($\sim 0.8''$); in particular, based on the source low-frequency radio

properties, Massaro et al. (2013b) classified this source as a γ-ray blazar candidate. As shown in Figure 2c the featureless spectrum of WISEJ050558.78+611335.9 confirms its BZB nature.

3.4. WISEJ064459.38+603131.7

This source is the gamma-ray blazar candidate counterpart of the UGS 2FGLJ0644.6+6034 proposed by Massaro et al. (2013a). The USNO-B optical counterpart lying at $\sim 0.4''$ features magnitudes B1=19.44 mag, R1=19.03 mag, B2=19.33 mag, R2=18.23 mag and I2=18.28 mag, while the IR counterpart 2MASSJ06445937+6031318 ($\sim 0.1''$) features magnitudes J=16.923 mag, H=15.979 mag and K=15.371 mag. According to Paggi et al. (2013) this source is positionally consistent ($\sim 0.1''$) with the X-ray *Swift* source SWXRTJ064459.9+603132 with a $0.3 - 10$ keV unabsorbed flux $\sim 2.1 \times 10^{-13}$ erg cm^{-2} s^{-1}. This source does not feature any obvious radio counterpart in the NVSS survey (the source is outside FIRST and SUMSS footprints), therefore down to ~ 2.5 mJy; nevertheless, based on its position in the three dimensional WISE IR color space, this source has been selected by Massaro et al. (2013a) as a γ-ray blazar candidate. The spectrum of WISEJ064459.38+603131.7 presented in Figure 2d show an almost featureless continuum with narrow Mg II ($EW = 6.1 \pm 0.4$ Å), and a weak detection of narrow Hδ ($EW = 7 \pm 2$ Å) emission lines (probably affected by contamination from noise/cosmic rays). For completeness we also report a poorly significant detection of narrow Hβ ($EW = 4 \pm 2$ Å), Such a spectrum is reminiscent of weak emission line quasar spectra (see e.g., Shemmer et al. 2006, 2009, and references therein), and yielding $z = 0.3582 \pm 0.0008$.

3.5. J104939.34+154837.8

This source lies in the positional uncertainty region of the *Fermi* AGU 2FGLJ1049.4+1551. It is associated with the NVSS radio sources NVSSJ104939+154838 ($\sim 1.0''$) and FIRST (Becker,

White, & Helfand 1995) FIRSTJ104939.3+154837 ($\sim 0.3''$), and with the optical counterpart SDSSJ104939.35+154837.6, with magnitudes u=18.58 mag, g=18.11 mag, r=17.64 mag, i=17.36 mag and z=17.13 mag. Furthermore this source is associated with 2MASSJ10493935+1548374 ($\sim 0.4''$) with magnitudes H=14.899 mag and K=14.144 mag and J=15.622 mag. According to the selection method presented by Massaro et al. (2013c), the radio emission from this source and its position in the two dimensional WISE IR color space classify this source as a γ-ray blazar candidate. The spectrum of WISEJ104939.34+154837.8 presented in Figure 2e shows an almost featureless spectrum typical of BZBs, with two weak absorption lines consistent with Ca II H & K ($EW = 0.70 \pm 0.13$ Å and $EW = 0.60 \pm 0.10$ Å, respectively) located at observed wavelength of 5220.6 and 5266.7 Å. Given this identification, the estimated redshift for this source is $z = 0.3271 \pm 0.0003$.

3.6.   WISEJ022239.60+430207.8

D'Abrusco et al. (2013) selected WISEJ022239.60+430207.8 as the IR counterpart of 2FGLJ0222.6+4302, associated in the 2FGL and in the 2LAC catalogs (Ackermann et al. 2011; Nolan et al. 2012) with the blazar BZBJ0222+4302, also known as 3C66A. This is a well known TeV detected BZB, associated with the radio source NVSSJ022239+430208, with a long and debated redshift estimate history. In fact, a past tentative measurement of $z = 0.444$ (Miller, French, & Hawley 1978; Kinney et al. 1991) was based on the measurement of single, weak line (the optical spectrum is not published, see Landt & Bignall 2008). There have also been suggestions that 3C66A is a member of a cluster at $z \sim 0.37$ (Butcher et al. 1976; Wurtz et al. 1993, 1997), while a lower limit of $z > 0.096$ based on the expected equivalent widths of absorption features in the blazar host galaxy has been set by Finke et al. (2008), and an upper limit of $z < 0.58$ has been set by Yang & Wang (2010) comparing the measured and intrinsic VHE spectra due to extragalactic background light absorption. In the same way, an estimate for the blazar redshift of

$z = 0.34 \pm 0.05$ was found by Prandini et al. (2010). Recently, Furniss et al. (2013) making use of far-ultraviolet HST/COS spectra, evaluated for 3C66A a redshift range $0.3347 < z < 0.41$ at 99% confidence. The source WISEJ022239.60+430207.8 is associated with the IR counterpart 2MASSJ02223961+4302078 ($\sim 0.1''$), with magnitudes J=12.635 mag, H=11.880 mag and K=11.151 mag, while the closest source in the USNO-B catalog, at $\sim 0.1''$, has brightnesses of B1=15.88.44 mag, R1=15.15 mag, B2=14.94 mag, R2=14.35 mag and I2=12.59 mag. (Shaw et al. 2013) observed 3C66A with the Low Resolution Imaging Spectrograph at the W. M. Keck Observatory, producing a featureless spectra that did not yield a redshift estimate As shown in Figure 3a, WISEJ022239.60+430207.8 shows a similar featureless spectrum, typical of BZBs so, even if we are not able to obtain a spectroscopic redshift estimate, we confirm the blazar nature of WISEJ022239.60+430207.8, which therefore is the IR counterpart of 3C66A.

3.7. WISEJ100800.81+062121.2

D'Abrusco et al. (2013) selected this WISE source as the IR counterpart of the gamma-ray source 2FGLJ1007.7+0621 (Ackermann et al. 2011; Nolan et al. 2012), associated with the blazar candidate BZBJ1008+0621, associated with the radio sources NVSSJ100800+062121 and FIRSTJ100800.8+06212. The WISE source is also associated with a USNO-B source ($\sim 0.2''$) with brightnesses of B1=17.72 mag, R1=16.72 mag, B2=18.54 mag, R2=16.73 mag and I2=16.74 mag, and with the SDSS source SDSSJ100800.81+062121.2 ($\sim 0.1''$) with magnitudes u=18.65 mag, g=18.11 mag, r=17.64 mag, i=17.29 mag and z=17.02 mag; the associated optical spectrum shows weak emission lines yielding a QSO classification with a redshift estimate $z = 1.36456 \pm 0.00015$. The associated IR counterpart 2MASSJ10080081+0621212 ($\sim 0.1''$) has magnitudes J=14.121 mag, H=13.345 mag and K=12.458 mag, and has been classified by Urrutia et al. (2009) as an high variable blazar with $z = 1.72$ on the basis of optical spectroscopy performed with the ESI instrument of the W. M. Keck Observatory telescope. This is at variance

with the findings of (Shaw et al. 2013), that observed BZBJ1008+0621 with the Low Resolution
Imaging Spectrograph at the W. M. Keck Observatory obtaining a featureless spectrum without
a redshift estimate As shown in Figure 3b, WISEJ100800.81+062121.2 feature an almost
featureless spectrum with only a weak narrow absorption line that we tentatively identify as Mg
II, yielding a redshift estimate of $z = 0.6495$. Although the source variability can explain the
variations in magnitudes and spectral shape, it cannot explain the differences in redshift estimates.
A direct comparison with Urrutia et al. is however not possible because the authors did not
presented their observed spectrum, since their work mainly dealt with red quasars. Although
cannot firmly estimate the source redshift, our spectrum confirms the BZB nature of the WISE
source, which therefore is the IR counterpart of BZBJ1008+0621.

3.8. WISEJ131443.81+234826.7

This WISE source has been selected by D'Abrusco et al. (2013) as the IR counterpart of *Fermi*
source 2FGLJ1314.6+2348, associated with the blazar candidate BZBJ1314+2348 (Ackermann
et al. 2011; Nolan et al. 2012), associated with the radio sources NVSSJ131443+234827 and
FIRSTJ131443.8+234826 (Bourda et al. 2011; Petrov 2011; Linford et al. 2011, 2012). The WISE
source is associated with the IR source 2MASSJ13144382+2348267 ($\sim 0.1''$), with brightnesses
J=15.514 mag, H=14.688 mag and K=13.832 mag (Mao 2011). Its optical counterpart found in
the USNO-B catalog ($\sim 0.1''$) features magnitudes B1=17.05, R1=15.43 mag, B2=17.80 mag,
R2=17.06 mag and I2=16.15 mag, while the closest SDSS source is SDSSJ131443.80+234826.7
($\sim 0.1''$) with magnitudes u=17.55 mag, g=17.14 mag, r=16.80 mag, i=16.54 mag and
z=16.31 mag; the associated low S/N optical spectrum in SDSS DR10 shows a number of
lines yielding a QSO classification with redshift estimate $z = 2.05885 \pm 0.00065$, although the
SMALL_DELTA_CHI2 flag indicates that there is more than one template that fits the spectrum
(a feature most commonly seen in low S/N spectra). In addition we note that the SDSS DR9

spectrum led to a galaxy classification with an uncertain redshift estimate $z = 0.22561 \pm 0.23874$. BZBJ1314+2348 has been observed with the Low Resolution Imaging Spectrograph at the W. M. Keck Observatory (Shaw et al. 2013) without yielding a redshift estimate. As shown in Figure 3c, WISEJ131443.81+234826.7 features a similar featureless spectrum, typical of BZBs so, even if we are not able to obtain a spectroscopic redshift estimate, we confirm the blazar nature of WISEJ131443.81+234826.7, which therefore is the IR counterpart of BZBJ1314+2348.

3.9. WISEJ172535.02+585140.0

D'Abrusco et al. (2013) found this WISE source to be the counterpart of the *Fermi* source 2FGLJ1725.2+5853, associated in the 2FGL and 2LAC catalogs (Ackermann et al. 2011; Nolan et al. 2012) with the BZB candidate BZBJ1725+5851 (Massaro et al. 2013). This WISE source is also associated with the radio sources NVSSJ172535+585139 ($\sim 0.8''$), FIRSTJ172535.0+585139 ($\sim 0.3''$) and WN1724.8+5854 ($\sim 2.2''$). The closest USNO-B source ($\sim 0.3''$) has brightnesses of B1=17.56 mag, R1=16.54 mag, B2=17.14 mag, R2=16.15 mag and I2=15.47 mag, while the closest SDSS source is SDSSJ172535.01+585139.9 ($\sim 0.2''$) with magnitudes u=18.38 mag, g=17.90 mag, r=17.55 mag, i=17.27 mag and z=17.00 mag. The associated IR source 2MASSJ17253500+5851400 ($\sim 0.1''$) has brightnesses J=15.549 mag, H=14.705 mag and K=13.952 mag. Our optical spectrum of WISEJ172535.02+585140.0, is presented in Figure 3d; it shows a featureless spectrum typical of BZBs. This supports our identification of WISEJ172535.02+585140.0 as the likely counterpart of BZBJ1725+5851. The other optical-IR sources nearby to the WISE position are SDSSJ172535.03+585140.0 ($\sim 0.1''$) and SSTXFLSJ172535.0+585139 ($\sim 0.1''$). (Richards et al. 2004) and (Marleau et al. 2007), report that these source are counterparts of 2MASSJ17253500+5851400, but while the former authors indicate for this source a photometric redshift estimate of $z = 2.025$ with a 53.3% probability of the source redshift lying in the range $2.00 < z < 2.20$, the latter authors report

a tentative redshift upper limit $z < 0.2974$ estimated from the 4000 Å break. While the latter estimate is compatible with our evidence of this source being a BZB (redshift of BZB in BZCAT range from 0.023 to 1.34, peaking at $z \sim 0.3$), the former is unlikely for such a source, indicating either a doubtful association of SDSSJ172535.03+585140.0 with 2MASSJ17253500+5851400 (or of the 2MASS source with WISEJ172535.02+585140.0) or an unreliable photometric redshift estimate.

4. Discussion

The optical spectra we obtained with MMT, Loiano and OAN telescopes provide the first confirmation of the association procedure and the tentative classification of gamma-ray blazar candidates developed by D'Abrusco et al. (2013) and adopted by Massaro et al. (2013a), as well as those proposed in Massaro et al. (2013b), Paggi et al. (2013) and Massaro et al. (2013c).

The four WISE sources associated with known γ-ray blazar counterparts have been tentatively classified as BZBs by D'Abrusco et al. (2013). In fact, the authors assign to every source a class A, B, or C depending on the probability of the WISE source to be compatible with the model of the WISE *Fermi* Blazar locus (WFB) in the three dimensional color space: class A sources are considered the most reliable candidate blazars for the high-energy source, while class B and class C sources are less compatible with the WFB locus but are still deemed as gamma-ray blazar candidates. According to this classification, the source WISEJ022239.60+430207.8 is a class A BZB γ-ray candidate, while the other sources here analyzed are class B BZBs. The spectra presented in Figure 3 confirm for all these sources their BZB nature. In addition, for the source WISEJ100800.81+062121.2 (associated with the blazar BZBJ1008+0621) we provide for the first time a tentative redshift estimate $z = 0.65$.

In addition, optical spectroscopy can be used to test the predictions of the different

association procedure that are used to find γ-ray blazar candidates lying in the uncertainty regions at 95% level of confidence of UGSs or AGUs listed in the 2FGL or 2LAC. In particular the sources WISEJ050558.78+611335.9 and WISEJ064459.38+603131.7 are selected by Massaro et al. (2013a) as class C γ-ray blazar candidates of BZB and undefined type, respectively; WISEJ060102.86+383829.2 is selected as γ-ray blazar candidate by Massaro et al. (2013b) on the basis of its low-frequency radio properties; WISEJ022051.24+250927.6 is selected as γ-ray blazar candidate by Paggi et al. (2013) combining its *Swift* X-ray emission and its IR WISE colors; finally, WISEJ104939.34+154837.8 is selected as γ-ray blazar candidate by Massaro et al. (2013c) combining its radio emission and its IR WISE colors. As shown in Figure 2 all these WISE sources show a blazar-like optical spectrum.

In particular, WISEJ050558.78+611335.9 and WISEJ060102.86+383829.2 show featureless BZB spectra, while WISEJ104939.34+154837.8 shows an almost featureless spectrum with weak absorption lines consistent with Ca II H & K yielding a redshift estimate $z = 0.33$; the EW of these line - 0.7 Å - is however consistent with the BZB definition given in Sect. 1.

On the other hand, WISEJ022051.24+250927.6 and WISEJ064459.38+603131.7 show BZQ type spectra with emission lines with $EW \sim 30$ Å and $EW \sim 6$ Å, yielding redshift values of $z = 0.48$ and $z = 0.36$, respectively. The spectrum of WISEJ064459.38+603131.7, in particular, is somewhat reminiscent of weak emission line quasar spectra (Shemmer et al. 2006, 2009), but the blazar identification for this source appears problematic. In fact the WISEJ064459.38+603131.7 is not detected by NVSS survey, so we can only put an upper limit on its flux ~ 2.5 mJy. Even if it is possible that deeper radio observations will detect emission from the source, blazars are traditionally defined as radio-loud sources basing on present radio data. All confirmed blazar from BZCAT are in fact detected at 1.4 GHz with fluxes $\gtrsim 1$ mJy, and radio-quiet blazars are extremely rare objects (Londish et al. 2004). Given the observed optical and X-ray flux and assuming $z = 0.36$ we can evaluate the effective spectral indices defined between the rest-frame frequencies

of 5 GHz, 5000 Å and 1 keV (e.g., Giommi et al. 1999), and put an upper limit on $\alpha_{ro} < 0.34$ and $\alpha_{rx} < 0.62$, while we have $\alpha_{ox} = 1.21$. We note that $\sim 25\%$ of the BZBs in BZCAT catalog have α_{ro} and α_{rx} smaller than the evaluated upper limits. However, these values are similar to the peak of the spectral index distributions found in the same catalog, that fall in the ranges $0.4 < \alpha_{ro} < 0.5$, $0.6 < \alpha_{rx} < 0.7$ and $1.2 < \alpha_{ox} < 1.3$.

The blazar nature of our candidates is also reinforced when comparing their multi-wavelength SEDs with those of the known γ-ray blazars, presented in Figures 4 and 5 in Appendix A, respectively. Despite the non simultaneity of the observations, we can clearly see the two main spectral components - that is, lower energy synchrotron and higher energy inverse Compton - typical of blazar SEDs. In the same figures we overplotted the optical spectra presented in Figures 2 and 3. Although a blazars are characterized by strong variability - and therefore a precise matching between non simultaneous data is not to be expected - we notice a general agreement between optical photometric and spectroscopic data.

5. Conclusions

We presented a pilot project to assess the effectiveness of several methods in selecting gamma-ray blazar candidates. To this end, we presented optical spectroscopic observations for a sample of five γ-ray blazar candidates selected with different methods based on their radio to IR properties, and for a sample of four WISE counterparts to known γ-ray blazar.

The main results of our analysis are summarized as follows:

1. We confirm the blazar nature of all the sources associated with known γ-ray blazars. In addition, we obtain for the first time a tentative redshift estimate $z = 0.65$ for the blazar BZBJ1008+0621.

2. We confirm the blazar nature of all the γ-ray blazar candidates selected by Massaro et

– 20 –

al. (2013a), Massaro et al. (2013b), Paggi et al. (2013) and Massaro et al. (2013c). In addition, we obtain for WISEJ104939.34+154837.8, WISEJ022051.24+250927.6 and WISEJ064459.38+603131.7 redshift estimates of $z = 0.33$, $z = 0.48$ and $z = 0.36$, respectively.

3. The source WISEJ064459.38+603131.7, in particular, is intriguing since it shows an almost featureless continuum with weak emission lines reminiscent of weak emission line quasar spectra (Shemmer et al. 2006, 2009), but it lacks any obvious radio counterpart, which is required for a blazar classification (Giommi et al. 2012; Giommi, Padovani, & Polenta 2013).

While these preliminary results seem to confirm the effectiveness of the classification method presented by D'Abrusco et al. (2013) and of the selection methods presented by Massaro et al. (2013a), Massaro et al. (2013b), Paggi et al. (2013) and Massaro et al. (2013c), additional ground-based, optical and near IR, spectroscopic follow up observations of a larger sample of γ-ray blazar candidates are needed to confirm the nature of the selected sources and to obtain their redshift.

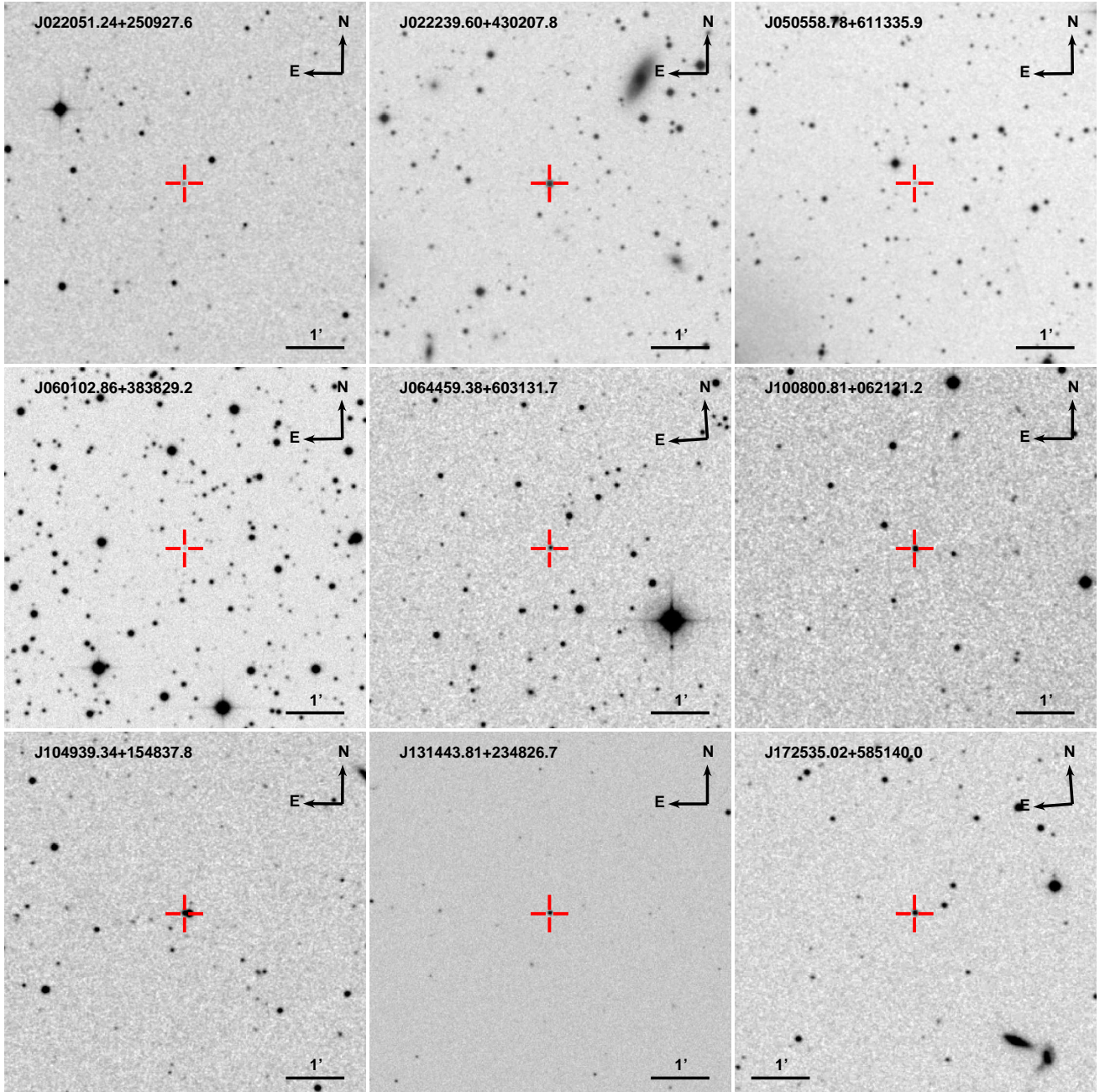[3]http://www.star.bris.ac.uk/~mb t/topcat/

Fig. 1.— Optical images of the fields of 9 of the WISE sources selected in this paper for optical spectroscopic follow-up (see Table 1). The object name, image scale and orientation are indicated in each panel. The proposed optical counterparts are indicated with red marks and the fields are extracted from the DSS-II-Red survey.

Table 2: Main observation properties of WISE sources discussed in this paper. For each source we indicate the name (WISE NAME), the date of the observation (OBS. DATE), the telescope used for the observations (TELESCOPE), the exposure time (EXPOSURE), the rest frame EW of the identified lines (EW), and the estimated redshift (REDSHIFT).

| WISE NAME	OBS. DATE	TELESCOPE	EXPOSURE (min)	EW (Å)									REDSHIFT
				Mg $\scriptstyle\rm II$	[Ne v]	[O $\scriptstyle\rm II$]	[Ne $\scriptstyle\rm III$]	Ca $\scriptstyle\rm II$ H	Ca $\scriptstyle\rm II$ K	H δ	H β	[O $\scriptstyle\rm III$]	
J022051.24+250927.6	2013-01-17	MMT	2×30	30.8 ± 0.7	1.8 ± 0.3	1.7 ± 0.3	1.1 ± 0.4	-	-	-	-	15.8 ± 0.3	0.4818 ± 0.0002
J050558.78+611335.9	2013-01-18	MMT	2×30	-	-	-	-	-	-	-	-	-	-
J060102.86+383829.2	2013-01-18	MMT	2×45	-	-	-	-	-	-	-	-	-	-
J064459.38+603131.7	2013-01-18	MMT	2×30	6.1 ± 0.4	-	-	-	-	-	7 ± 2	4 ± 2	-	0.3582 ± 0.0008
J104939.34+154837.8	2013-05-02	OAN	3×30	-	-	-	-	0.7 ± 0.1	0.6 ± 0.1	-	-	-	0.3271 ± 0.0003
J022239.60+430207.8	2012-12-03	Loiano	2×30	-	-	-	-	-	-	-	-	-	-
J100800.81+062121.2	2013-01-17	MMT	2×30	-	-	-	-	-	-	-	-	-	0.6495*
J131443.81+234826.7	2013-01-17	MMT	2×30	-	-	-	-	-	-	-	-	-	-
J172535.02+585140.0	2013-01-17	MMT	2×30	-	-	-	-	-	-	-	-	-	-

Notes:

* Tentative estimate.
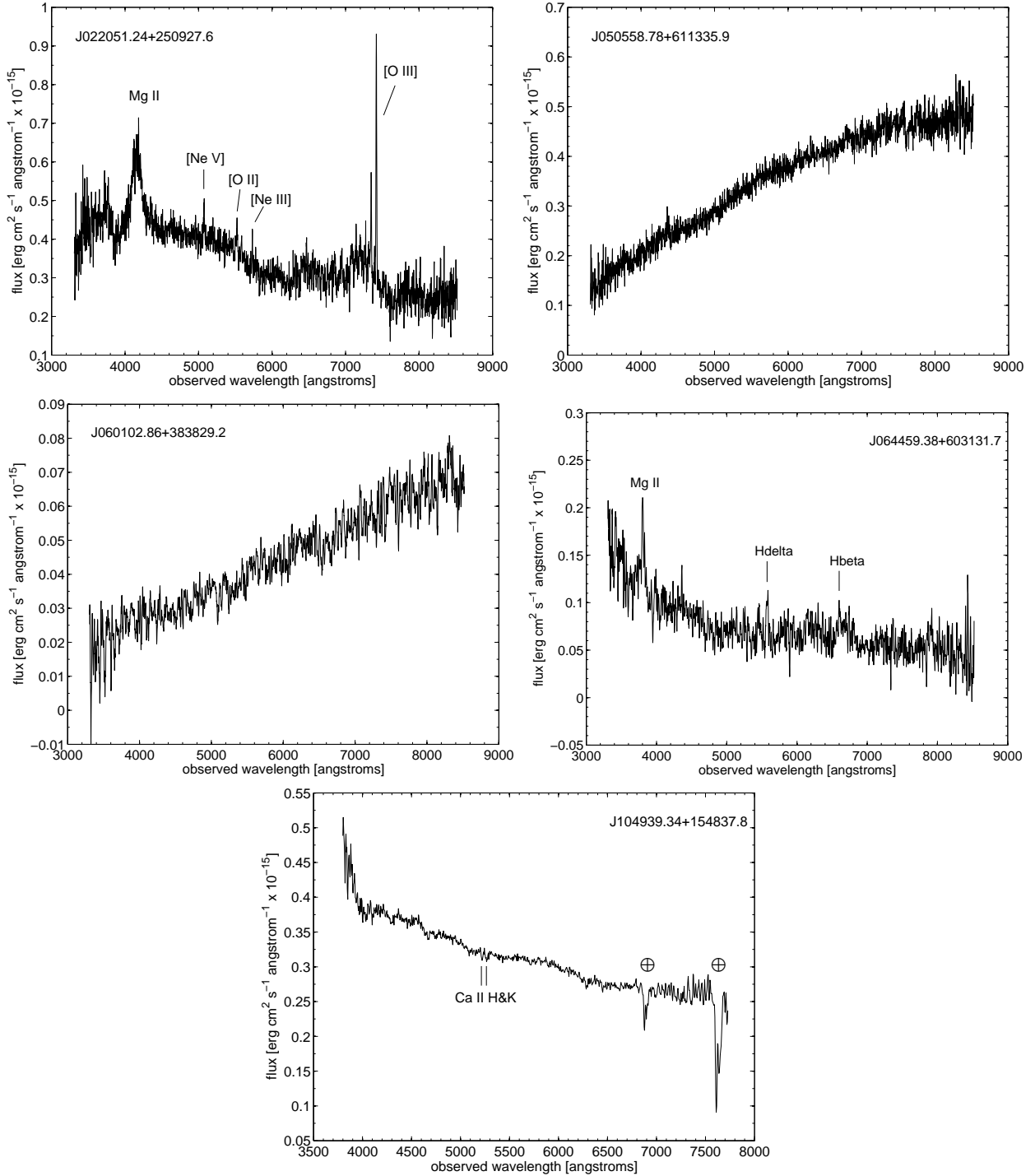
Fig. 2.— Optical spectra of the five WISE γ-ray blazar candidates associated with *Fermi*-LAT UGS or AGU. The WISE name of each source is indicated in the relative panel, as well as the identified emission lines. With the exception of J104939.34+154837.8, whose spectrum has been obtained with OAN telescope, all other spectra have been obtained with MMT Blue Channel Spectrograph.

Fig. 3.— Optical spectra of the four WISE sources associated by D'Abrusco et al. (2013) with known *Fermi*-LAT γ-ray blazars. As in Fig. 2, the WISE name of each source is indicated in the relative panel, as well as the identified emission lines. With the exception of J022239.60+430207.8, whose spectrum has been obtained with Loiano telescope, all other spectra have been obtained with MMT Blue Channel Spectrograph.
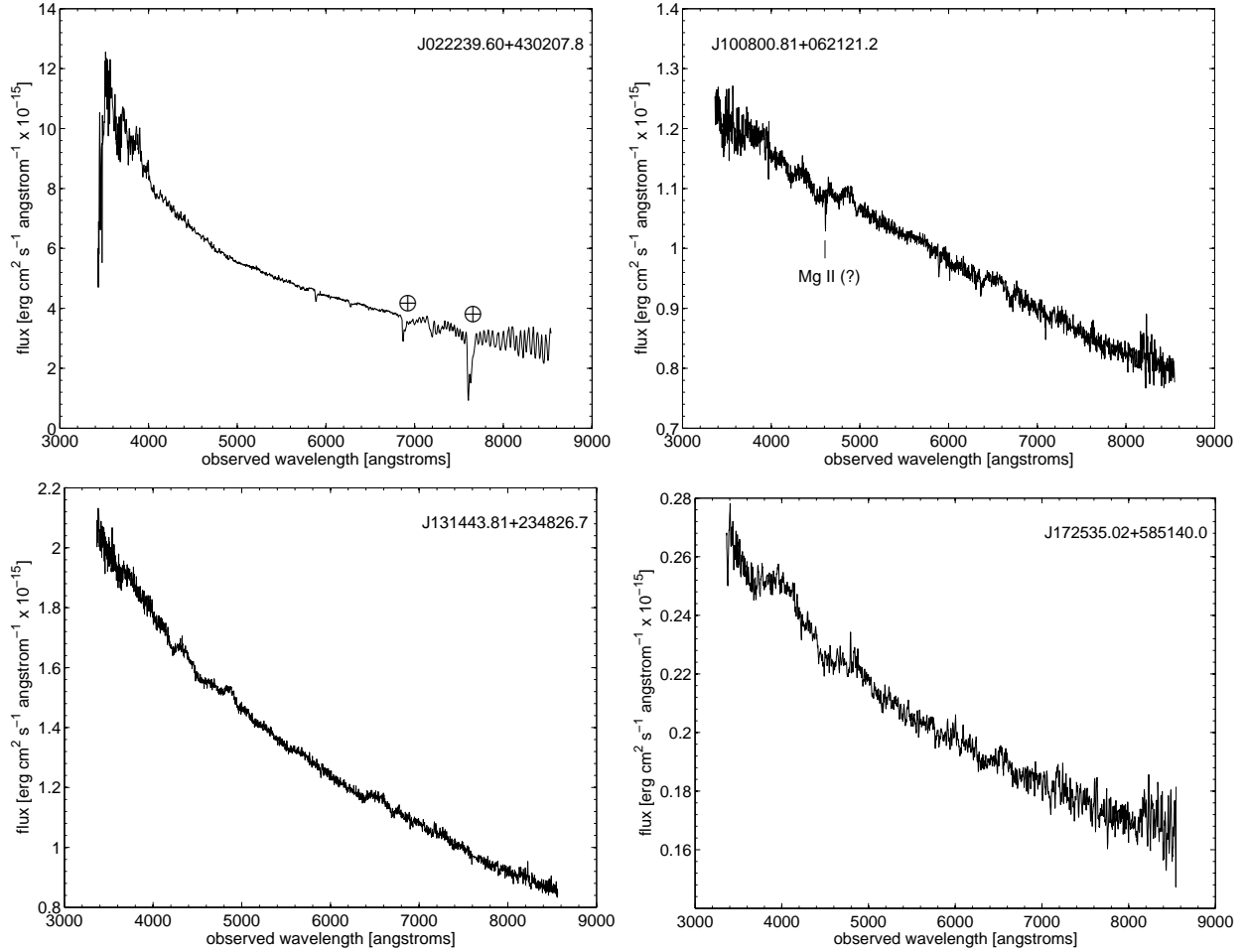
REFERENCES

Abdo A. A, et al., 2013, in preparation

Ackermann M., et al., 2011, ApJ, 743, 171

Aharonian F., et al., 2009, A&A, 502, 749

Ahn, C. P., Alexandroff, R., Allende Prieto, C., et al. 2013, arXiv:1307.7735

Arnaud K. A., 1996, ASPC, 101, 17

Bauer, A., Baltay, C., Coppi, P., et al. 2009, ApJ, 705, 46

Becker R. H., White R. L., Helfand D. J., 1995, ApJ, 450, 559

Blandford R. D., Rees M. J., 1978, Proc. "Pittsburgh Conference on BL Lac objects", 328

Bourda G., Collioud A., Charlot P., Porcas R., Garrington S., 2011, A&A, 526, A102

Brand, K., Brown, M. J. I., Dey, A., et al. 2006, ApJ, 641, 140

Butcher H. R., Oemler A., Jr., Tapia S., Tarenghi M., 1976, ApJ, 209, L11

Capalbi M., Perri M. Saija B. Tamburelli F., Angelini L. 2005, http://heasarc.nasa.gov/docs/swift/analysis/xrt swguide v1 2.pdf

Cardelli J. A., Clayton G. C., Mathis J. S., 1989, ApJ, 345, 245

Condon J. J., Cotton W. D., Greisen E. W., Yin Q. F., Perley R. A., Taylor G. B., Broderick J. J., 1998, AJ, 115, 1693

Cowperthwaite P. S., Massaro F., D'Abrusco R., Paggi A., Tosti G., Smith H. A., 2013, arXiv, arXiv:1308.1950

D'Abrusco R., Longo G., Walton N. A., 2009, MNRAS, 396, 223

D'Abrusco R., Massaro F., Ajello M., Grindlay J. E., Smith H. A., Tosti G., 2012, ApJ, 748, 68

D'Abrusco R., Massaro F., Paggi A., Masetti N., Tosti G., Giroletti M., Smith H. A., 2013, ApJS, 206, 12

D'Elia V., et al., 2013, A&A, 551, A142

Dermer C. D., Schlickeiser R., 1993, ApJ, 416, 458

Dermer C. D., Finke J. D., Krug H., Böttcher M., 2009, ApJ, 692, 32

Fermi collaboration, 2013, ApJ, in preparation

Finke J. D., Shields J. C., Böttcher M., Basu S., 2008, A&A, 477, 513

Freeman P., Doe S., Siemiginowska A., 2001, SPIE, 4477, 76

Fruscione A., et al., 2006, SPIE, 6270

Furniss A., Fumagalli M., Danforth C., Williams D. A., Prochaska J. X., 2013, ApJ, 766, 35

Giommi, P., Menna, M. T., & Padovani, P. 1999, MNRAS, 310, 465

Giommi P., Padovani P., Polenta G., Turriziani S., D'Elia V., Piranomonte S., 2012, MNRAS, 420, 2899

Giommi P., Padovani P., Polenta G., 2013, MNRAS, 431, 1914

Inoue S., Takahara F., 1996, ApJ, 463, 555

Kalberla P. M. W., Burton W. B., Hartmann D., Arnal E. M., Bajaja E., Morras R., Pöppel W. G. L., 2005, A&A, 440, 775

Kinney A. L., Bohlin R. C., Blades J. C., York D. G., 1991, ApJS, 75, 645

Landoni, M., Falomo, R., Treves, A., et al. 2012, A&A, 543, A116

Landoni, M., Falomo, R., Treves, A., et al. 2013, AJ, 145, 114

Landt H., Bignall H. E., 2008, MNRAS, 391, 967

Laurent-Muehleisen S. A., Kollgaard R. I., Feigelson E. D., Brinkmann W., Siebert J., 1999, ApJ, 525, 127

Laurino O., D'Abrusco R., Longo G., Riccio G., 2011, MNRAS, 418, 2165

Linford J. D., et al., 2011, ApJ, 726, 16

Linford J. D., Taylor G. B., Romani R. W., Helmboldt J. F., Readhead A. C. S., Reeves R., Richards J. L., 2012, ApJ, 744, 177

Londish D., Heidt J., Boyle B. J., Croom S. M., Kedziora-Chudczer L., 2004, MNRAS, 352, 903

Mao L. S., 2011, NewA, 16, 503

Marleau F. R., Fadda D., Appleton P. N., Noriega-Crespo A., Im M., Clancy D., 2007, ApJ, 663, 218

Massaro, E., Giommi, P., Leto, C., et al. 2013, VizieR Online Data Catalog, 349, 50691

Massaro F., D'Abrusco R., Ajello M., Grindlay J. E., Smith H. A., 2011b, ApJ, 740, L48

Massaro F., D'Abrusco R., Tosti G., Ajello M., Gasparrini D., Grindlay J. E., Smith H. A., 2012a, ApJ, 750, 138

Massaro F., D'Abrusco R., Paggi A., Masetti N., Giroletti M., Tosti G., Smith H. A., Funk S., 2013a, ApJS, 206, 13

Massaro F., D'Abrusco R., Giroletti M., Paggi A., Masetti N., Tosti G., Nori M., Funk S., 2013b, ApJS, 207, 4

Massaro, F., D'Abrusco, R., Paggi, A., et al. 2013c, ApJS, 209, 10

Matheson, T., et al., 2008, AJ, 135, 1598

Miller J. S., French H. B., Hawley S. A., 1978, bllo.conf, 176

Monet D. G., et al., 2003, AJ, 125, 984

Moretti A., et al., 2005, SPIE, 5898, 360

Nolan P. L., et al., 2012, ApJS, 199, 31

Paggi, A., Massaro, F., D'Abrusco, R., et al. 2013, ApJS, 209, 9

Pâris I., et al., 2012, A&A, 548, A66

Perri M., et al., 2007, A&A, 462, 889

Petrov L., 2011, AJ, 142, 105

Prandini E., Bonnoli G., Maraschi L., Mariotti M., Tavecchio F., 2010, MNRAS, 405, L76

Puccetti S., et al., 2011, A&A, 528, A122

Rengelink R. B., Tang Y., de Bruyn A. G., Miley G. K., Bremer M. N., Roettgering H. J. A.,
     Bremer M. A. R., 1997, A&AS, 124, 259

Richards G. T., et al., 2004, ApJS, 155, 257

Sbarufatti, B., Treves, A., Falomo, R., et al. 2006, AJ, 132, 1

Sbarufatti, B., Ciprini, S., Kotilainen, J., et al. 2009, AJ, 137, 337

Shaw M. S., et al., 2013, ApJ, 764, 135

Shemmer O., et al., 2006, ApJ, 644, 86

Shemmer O., Brandt W. N., Anderson S. F., Diamond-Stanic A. M., Fan X., Richards G. T.,
     Schneider D. P., Strauss M. A., 2009, ApJ, 696, 580

Skrutskie M. F., et al., 2006, AJ, 131, 1163

Stickel M., Padovani P., Urry C. M., Fried J. W., Kuehr H., 1991, ApJ, 374, 431

Stocke J. T., Rector T. A., 1997, ApJ, 489, L17

Taylor M. B., 2005, ASPC, 347, 29

Urrutia T., Becker R. H., White R. L., Glikman E., Lacy M., Hodge J.,Gregg M. D., 2009, ApJ, 698, 1095

Urry C. M., Padovani P., 1995, PASP, 107, 803

Wright E. L., et al., 2010, AJ, 140, 1868

Wurtz R., Ellingson E., Stocke J. T., Yee H. K. C., 1993, AJ, 106, 869

Wurtz R., Stocke J. T., Ellingson E., Yee H. K. C., 1997, ApJ, 480, 547

Yang J., Wang J., 2010, PASJ, 62, L23

A. SEDs

SEDs of the sources listed in Table 1 are presented in Figures 4 and 5. For each source we show the spectral points corresponding to the various counterparts we found in a standard 3.3″ searching radius (see D'Abrusco et al. 2013). Circles represent detections, while down triangles represent upper limits, with the color code presented in the legends. For IR, optical and UV points we present de-reddened fluxes obtained using the extinction law presented by Cardelli, Clayton, & Mathis (1989) and the galactic extinction value as derived by the Infrared Science Archive[4] (IRSA). The XRT data were processed using the XRTDAS software (Capalbi et al. 2005) developed at the ASI Science Data Center and included in the HEAsoft package (v. 6.13) distributed by HEASARC. For each observation of the sample, calibrated and cleaned PC mode event files were produced with the XRTPIPELINE task (ver. 0.12.6), producing exposure maps for each observation. In addition to the screening criteria used by the standard pipeline processing, we applied a further filter to screen background spikes that can occur when the angle between the pointing direction of the satellite and the bright Earth limb is low. In order to eliminate this so called bright Earth effect, due to the scattered optical light that usually occurs towards the beginning or the end of each orbit, we used the procedure proposed by Puccetti et al. (2011) and D'Elia et al. (2013). We monitored the count rate on the CCD border and, through the XSELECT package, we excluded time intervals when the count rate in this region exceeded 40 counts/s; moreover, we selected only time intervals with CCD temperatures less than -50°C (instead of the standard limit of -47°C) since contamination by dark current and hot pixels, which increase the low energy background, is strongly temperature dependent (D'Elia et al. 2013). We then proceeded to merge cleaned event files obtained with this procedure using XSELECT, considering only observations with telescope aim point falling in a circular region of 10' radius centered in the median of the individual aim points, in order to have a uniform exposure. The corresponding

---

[4]http://irsa.ipac.caltech.edu/ap plications/DUST/

merged exposure maps were then generated by summing the exposure maps of the individual observations with XIMAGE (ver. 4.5.1). When possible, *Swift* XRT-PC spectra are obtained form merged events extracted with XRTPRODUCTS task using a 20 pixel radius circle centered on the coordinates reported in Table 1 and background estimated from a nearby source-free circular region of 20 pixel radius. When the source count rate is above 0.5 counts s^{-1}, the data are significantly affected by pileup in the inner part of the point-spread function (Moretti et al. 2005). To remove the pile-up contamination, we extract only events contained in an annular region centered on the source (e.g., Perri et al. 2007). The inner radius of the region was determined by comparing the observed profiles with the analytical model derived by Moretti et al. (2005) and typically has a 4 or 5 pixels radius, while the outer radius is 20 pixels for each observation. Source spectra are binned to ensure a minimum of 20 counts per bin in order to ensure the validity of χ^2 statistics. We performed our spectral analysis with the SHERPA[5] modeling and fitting application (Freeman, Doe, & Siemiginowska 2001) include in the CIAO (Fruscione et al. 2006) 4.5 software package, and with the XSPEC software package, version 12.8.0 (Arnaud 1996) with identical results. For the spectral fitting we used a model comprising an absorption component fixed to the Galactic value (Kalberla et al. 2005) and a powerlaw, and we plot intrinsic fluxes (i.e., without Galactic photoelectric absorption). When the extracted counts are not enough to provide acceptable spectral fits we simply converted the extracted count rates to 0.3-10 keV intrinsic fluxes with PIMMS[6] 4.6b software, assuming a powerlaw spectra with spectral index 2 and an absorption component fixed to the Galactic value, and in this case we report with a filled circle the flux corresponding to the extracted countrate.

---

[5]http://cxc.harvard.edu/sherpa

[6]http://heasarc.nasa.gov /docs/journal/pimms3.html

Fig. 4.— SEDs of γ-ray blazar candidates listed in the upper part of Table 1. Circles represent detections, while down triangles represent upper limits. In black we overplot the optical spectra presented in Figures 2 (magnified in the insets).
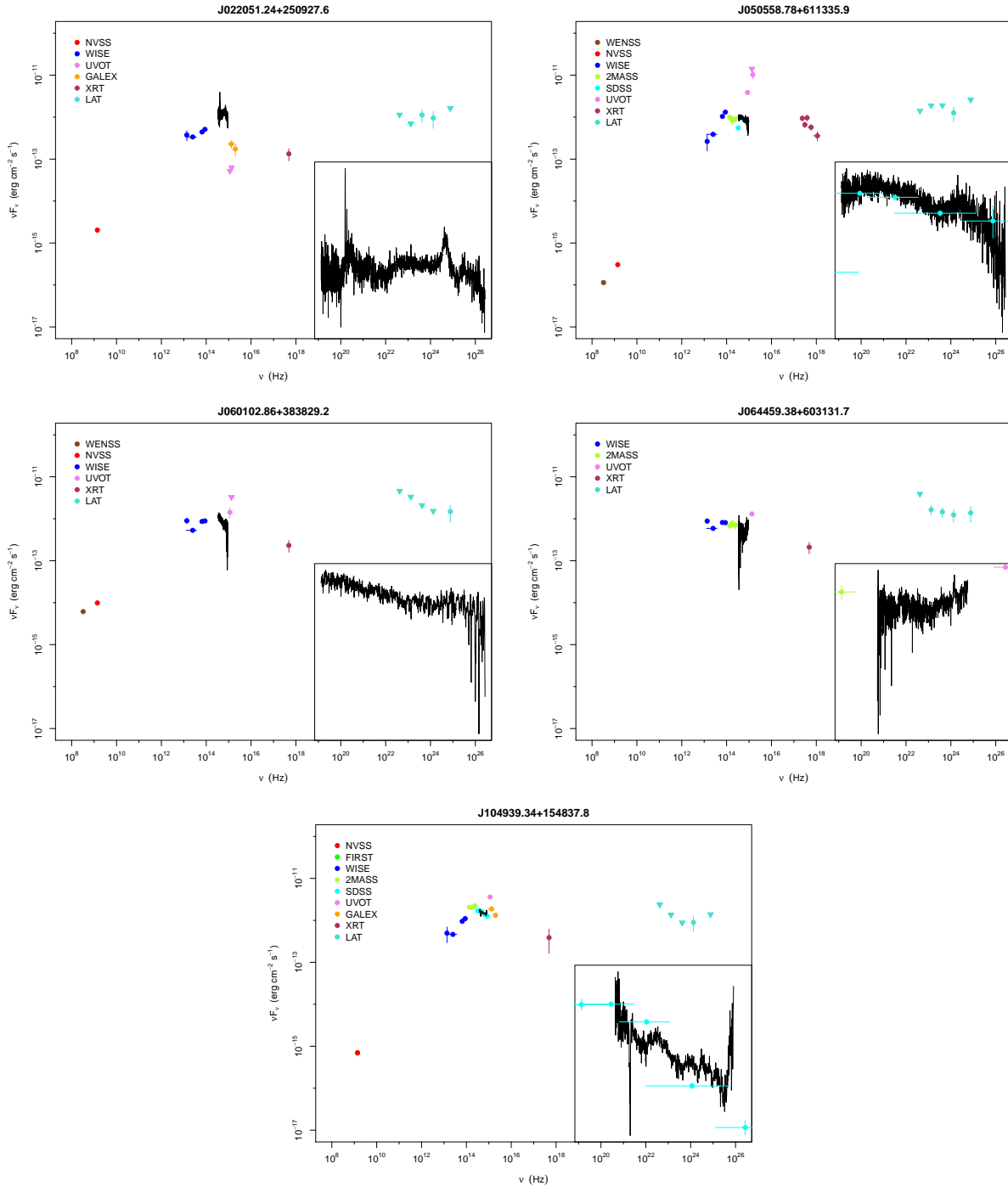
Fig. 5.— SEDs of γ-ray blazar candidates listed in the lower part of Table 1. Circles represent detections, while down triangles represent upper limits. In black we overplot the optical spectra presented in Figures 3 (magnified in the insets).